The Motion of Trapped Holes on Nanocrystal Surfaces

James Utterback, R. Peyton Cline, Katherine Shulenberger, Joel Eaves, Gordana Dukovic

Temperature-Dependent Transient Absorption Spectroscopy Elucidates Trapped-Hole Dynamics in CdS and CdSe Nanorods

*James K. Utterback, Jesse L. Ruzicka, Hayden Hamby, Joel D. Eaves, Gordana Dukovic**
Department of Chemistry, University of Colorado Boulder, Boulder, Colorado 80309, USA

Corresponding Author
* E-mail: gordana.dukovic@colorado.edu

ABSTRACT

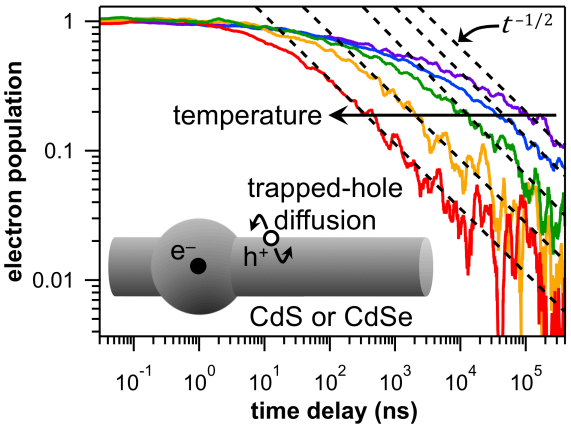

Charge-carrier traps play a central role in the excited-state dynamics of semiconductor nanocrystals, but their influence is often difficult to measure directly. In CdS and CdSe nanorods of nonuniform width, spatially-separated electrons and trapped holes display recombination dynamics that follow a power-law function in time that is consistent with trapped-hole diffusion-limited recombination. However, power-law relaxation can originate from mechanisms other than diffusion. We report transient absorption spectroscopy measurements on CdS and CdSe nanorods recorded at temperatures ranging from 160 to 294 K. We find that the exponent of the power law is temperature-independent, which rules out several models based on stochastic activated processes and provides insights into the mechanism of diffusion-limited recombination in these structures. The data point to weak electronic coupling between trap states and that surface-localized trapped holes couple strongly to phonons, leading to slow diffusion. Trap-to-trap hole hopping behaves classically near room temperature while quantum aspects of phonon-assisted tunneling become observable at low temperatures.

MAIN TEXT

Although colloidal semiconductor nanocrystals have been widely studied for three decades,[1,2] the understanding of their excited-state dynamics continues to evolve. The presence of charge-carrier trap states on nanocrystal surfaces leads to rich and complex excited-state relaxation.[3-13] Trap states play an essential role in processes such as electron–hole recombination and charge transfer,[4,6,7,14-16] yet their dynamics are challenging to probe spectroscopically.[17,18] Photogenerated holes in CdS and CdSe nanocrystals trap to the orbitals of undercoordinated S and Se atoms on the particle surface on a picosecond timescale.[3,8,17-21] Thus, electrons in these structures recombine primarily with holes that are localized to the surface, rather than delocalized in the valence band.[17,18]

We recently presented evidence that trapped holes on the surfaces of CdS and CdSe nanocrystals are not stationary but instead undergo a diffusive random walk at room temperature.[10-13,16] This evidence came from transient absorption (TA) spectroscopy measurements of recombination dynamics between spatially separated electrons and trapped holes in nonuniform CdS and CdSe nanorods (NRs). At long times, the TA signal associated with this recombination follows a robust and reproducible power law in time with an exponent of –1/2. We interpreted this behavior as the signature of diffusion-limited recombination in one dimension, where a trapped hole undergoes an unbiased random walk along the NR surface, with steps on the order of interatomic distances, until it reaches the electron and recombines.[10] Subsequent theoretical work used detailed electronic structure calculations to characterize the surface traps in CdS and found that, near room temperature, the trapped holes hop nonadiabatically between localized sulfur orbitals on the surface.[13]

There are, however, other mechanisms that can lead to power-law excited-state relaxation in nanocrystals. In particular, to model nonexponential relaxation dynamics in nanocrystals, researchers have often invoked stochastic rate theories, where there is a distribution of relaxation rates in the ensemble. Examples include electron trapping with a distribution in activation barrier heights[22] and charge-carrier detrapping with a distribution in trap depths.[23-25] An experimental method is needed to differentiate between these mechanisms and diffusion-limited recombination in nonuniform NRs.

The key measurable difference between the trapped-hole diffusion model and the alternative models listed above lies in the temperature dependence of the power-law exponent. In the one-dimensional diffusion–annihilation model, the temperature dependence appears in the magnitude of the diffusion coefficient while the power-law exponent of –1/2 is uniquely determined by the geometry.[26] In contrast, models that involve thermally-activated processes give rise to temperature-dependent power-law exponents.[22,25] In this paper we present TA spectroscopy of solutions of CdS and CdSe NRs over a range of temperatures from 160 to 294 K. From these data, we extract the temperature dependence of the power-law exponent and provide an experimental method to definitively distinguish between diffusion-limited recombination and stochastic rate theories. In concert with the diffusion-limited recombination theory, these experiments inform on the mechanism of the diffusion process, providing measurements of both the electronic coupling between hole trap states and the trapped hole–phonon coupling. At high temperatures and weak electronic coupling, the reorganization energy alone quantifies the strength of the hole-phonon coupling.

Prior evidence for trapped-hole diffusion comes from TA spectroscopy of nonuniform nanorods of CdS and CdSe at room temperature.[10-12] Such NRs consist of narrow-diameter cylindrical “rods” and wide-diameter “bulbs” (Figure 1a,b and Figure S1).[10,12,27,28] The rod and bulb morphological features constitute spatially and spectrally distinct electronic states wherein charge carriers in the rod have higher energy than in the bulb due to differences in radial quantum confinement (Figure 1c).[10,12,28] As described previously in room-temperature TA studies,[10-12] trapped holes likely diffuse in nanostructures of uniform morphologies as well, but the spatial dynamics of trapped holes are revealed in these nonuniform NRs when holes rapidly trap on the rod surface and electrons dissociate from them and localize in the bulb so that recombination can only occur if the electron and trapped hole reach each other in some way.

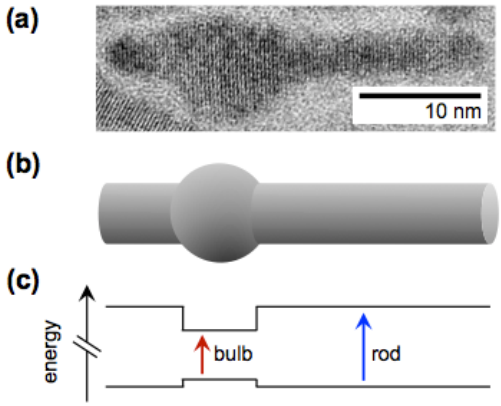

Figure 1. Morphology and energy-level diagram for nonuniform nanorods. (a) Selected transmission electron microscope image of a nonuniform CdS nanorod. (b) Schematic diagram of a nonuniform nanorod, depicting the rod and bulb components. (c) Energy-level diagram as a function of position along the nanorod, according to (b).

To carry out TA spectroscopy measurements at cryogenic temperatures, the NRs were functionalized with 3-mercaptopropanoic acid surface-capping ligands and suspended in a polar glass-forming mixture of 4:1 ethanol:methanol (v/v). Temperature was controlled using a cryostat purged with a nitrogen atmosphere, and experiments were limited to temperatures above the glass-transition temperature of the solution. Figure 2a,b show the TA spectra of CdS and CdSe NRs after excitation of the rod at temperatures ranging from 160 to 294 K. As temperature decreases, the bleach peaks shift to higher energies and become narrower, as is observed in bulk and nanocrystalline semiconductors (Figure S2).[29,30] The TA spectrum of nonuniform nanorods consists of distinct spectral features corresponding to the rod and the bulb states (Figure 2), the amplitudes of which predominantly reflect the population of electrons in each state.[10,12,27,28,31] The dynamics of electrons in the rod and bulb states were isolated and analyzed as described previously for room-temperature experiments (see Methods section and Section IV of the Supporting Information (SI)).[10,12] The data shown in Figure S3 indicate that sub-nanosecond spatial separation occurs at each temperature, leading to a charge-separated state where the electron is localized in the bulb and the hole is trapped on the surface of the rod (Figure 2c,d inset).

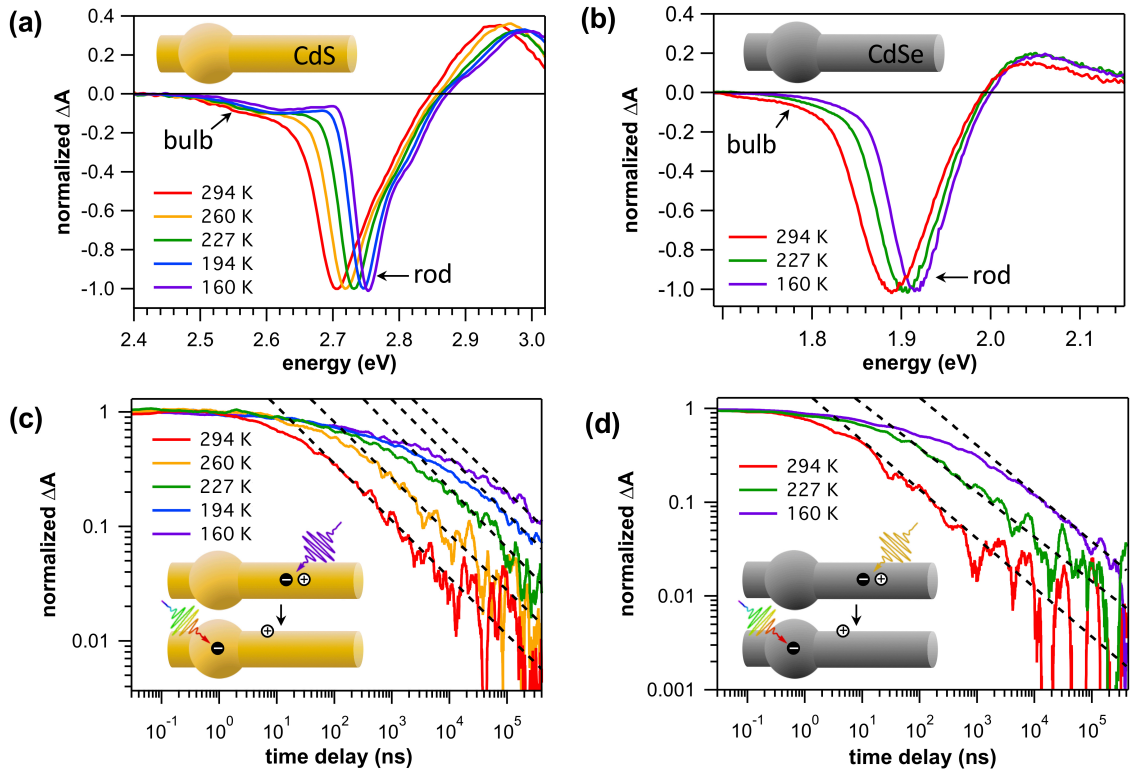

Figure 2. Temperature dependence of excited-state dynamics in CdS and CdSe nanorods. (a,b) Normalized TA spectra at different temperatures between 160 and 294 K of (a) CdS NRs averaged over 100–300 ns and (b) CdSe NRs averaged over 1–3 ns. CdS NRs were excited with 400 nm pulses and CdSe NRs were excited with 600 nm pulses. The parts of the bleach assigned to bulb and rod transitions are marked with arrows. (c,d) TA time traces of bulb bleach signal of (c) CdS NRs and (d) CdSe NRs normalized at 100 ps. Power-law tails were fit with an adjustable power-law exponent (black dashed lines). Data are smoothed for presentation. The insets of (c,d) depict the charge-separated state being probed after excitation of the rod.

To investigate the recombination dynamics of spatially separated electrons and trapped holes in CdS and CdSe NRs as a function of temperature, we monitor the decay of the TA bleach signal corresponding to the bulb electron population in the time window after charge separation at temperatures ranging from 160 to 294 K. Bulb decays for CdS NRs at five different temperatures are shown in Figure 2c, while the equivalent data for CdSe NRs at three different temperatures are shown in Figure 2d. At 294 K, both materials exhibit power-law decays at long times, consistent with previous observations.[10,12] As the temperature is lowered, the bulb electron relaxation gets slower but the power-law decay persists at every temperature. This is in contrast to the recombination kinetics in uniform NRs, which exhibit exponential tails at all temperatures in the range 160 to 294 K (Figure S4) due to direct recombination of spatially overlapping electrons and trapped holes.[10,12]

As we noted above, the temperature dependence of the exponent in a power-law decay can provide definitive insights into the mechanism of electron–hole recombination that leads to the power law. The tails of each decay in Figures 2c and 2d were fit to a power-law function of the form $S(t) \sim t^{-\alpha}$ (see Methods). The fit results are plotted in Figure 3. For every temperature studied, the power-law exponent is within experimental error of –1/2 for both CdS and CdSe NRs.

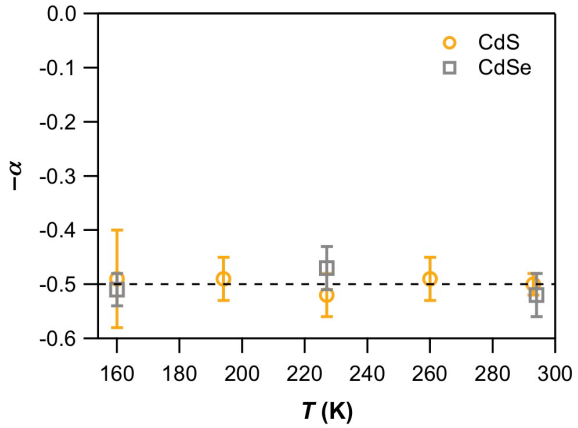

Figure 3. The extracted exponent of the power-law decay, $-\alpha$, in nonuniform CdS and CdSe NRs is independent of temperature.

The persistence of the power-law exponent of –1/2 over a broad range of temperatures in both CdS and CdSe NRs strongly supports the assignment of power-law recombination kinetics to diffusion-limited recombination between the bulb electron and a trapped hole. In this model, the trapped hole starts near the bulb and undergoes an unbiased random walk along the length of the rod until it encounters the stationary electron in the bulb and recombines with it.[10] Diffusion purely around the circumference of the rod does not contribute to decay of the bulb electron, so recombination is a one-dimensional process.[10] While temperature can change the diffusion coefficient, a power-law exponent of –1/2 is a universal feature of diffusion–annihilation in one dimension and is independent of temperature.[26]

The temperature independence of the power-law exponent allows us to rule out models in which there is a distribution in rate constants for recombination in an ensemble of particles. Power-law kinetics can arise in an ensemble of particles when their first-order rate constants reflect a thermally-activated process and there is an exponential distribution in the activation energies, $P(E_\mathrm{a}) = e^{-E_\mathrm{a}/\epsilon}/\epsilon$, where E_a is the activation energy and ϵ represents the mean barrier height, which is independent of temperature. In this case, the decay of the ensemble excited-state population goes as $S(t) \sim t^{-\alpha}$ at long times, where the power-law exponent $\alpha = k_\mathrm{B}T/\epsilon$ depends on temperature (T) as well as the material properties of the sample that determine ϵ, such as composition, size, and ligands.[22,25] There are several plausible scenarios in which the observed power-law decay of the bulb electron population could be due to such activated mechanisms. Electrons could trap from the bulb state while the trapped hole remains stationary on the rod,[10,32,33] in which case the power-law decay of the electron population would reflect a distribution in electron trapping rates,[34-36] which could originate from a distribution in trapping activation barriers.[22] Additionally, recombination could occur by thermal excitation of the electron from the bulb back to the rod where it would overlap directly with the trapped hole. In this case, a distribution of rate constants would reflect a distribution in relative rod and bulb radii. Finally, recombination could be limited by detrapping of the hole: a stationary trapped hole could eventually return to the valence band with a distribution of hole detrapping times that originates from a distribution in trap depths,[23-25] and from there it would rapidly transfer to the bulb where it would recombine with the electron.

Each of these mechanisms can be ruled out by the lack of temperature independence of the experimentally measured power-law exponent of the bulb electron decay (Figure 3). If the power-law tails observed in CdS and CdSe NRs in Figure 2 were due to an activated mechanism, α would

be proportional to temperature and would have changed by nearly a factor of two over the temperature range studied. Moreover, even though the distributed activated models could give rise to a power-law decay, one would expect α to be highly sensitive to sample preparation, because sample-to-sample variation is likely to cause significant changes in the value of ϵ in the distributions of, for example, the relative sizes of the rods and bulbs, electron trapping barriers or the hole trap depths. Not only is the power-law exponent temperature independent, it has proven to be robust and insensitive to many sample-dependent quantities. It has been measured in over twenty CdS NR samples to date, ZnSe/CdS and CdSe/CdS dot-in-rod heterostructures, and CdSe NRs.[10-12] The same exponent appears also for both native phosphonic acid ligands and mercaptocarboxylate ligands.[10] Thus, the temperature dependence data and the reproducibility of α favor a model in which the fundamental microscopic behavior is robust to sample variation and composition, depending only on a universal property of these systems, such as the dimensionality. Separately, we note that the notion of recombination via hole detrapping in our samples is inconsistent with the low photoluminescence quantum yields typically observed in CdS and CdSe nanocrystals,[4,37,38] which imply that electrons predominantly recombine with trapped holes rather than valence-band holes.[18] It is worth noting that the present work does not indicate that the above activated processes do not occur on some timescale, just that they do not dominate the mechanism behind the power-law decay of charge-separated electrons and trapped holes in CdS and CdSe NRs.

We next examine the temperature dependence of the trapped-hole hopping rate to gain insights into the nature of the trapped-hole diffusion mechanism. For a trapped hole that begins at a distance z_0 from the bulb and diffuses with diffusion coefficient D, the onset of the $t^{-1/2}$ power-law tail of the survival probability occurs on a timescale of approximately $\tau = z_0^2/4D$ (see Section VI of the SI).[10,26] The diffusion coefficient, in turn, is related to the step length of the random walk, a, and the hole-hopping rate, κ, by $D = a^2\kappa$.[13,26] For diffusion along the length of the nanorod, a is the lattice constant for the wurtzite c-axis and κ is the total hopping rate that is composed of chalcogenide-to-chalcogenide hole hopping steps that are both parallel with and diagonal to the wurtzite c-axis.[13] The extent of lattice contraction over the measured temperature range is negligible (~0.1%),[39] making a approximately constant with respect to temperature. We also assume that the initial distribution of trapped-hole positions does not change substantially with temperature. In this case, the temperature dependence of the observable τ is inversely proportional to the temperature dependence of the hole-hopping rate: $\tau^{-1}(T) = \frac{4D}{z_0^2} = \frac{4a^2}{z_0^2}\kappa(T)$. The data in Figure 2 allow us to extract the lower and upper bounds of τ, which yield bounds on the hole-hopping rates in CdS and CdSe nanorods. The procedure for extracting the bounds of τ is described in Section VI of the SI (Figure S5). Figure 4 shows the resulting range, displayed as an Arrhenius plot of τ^{-1}.

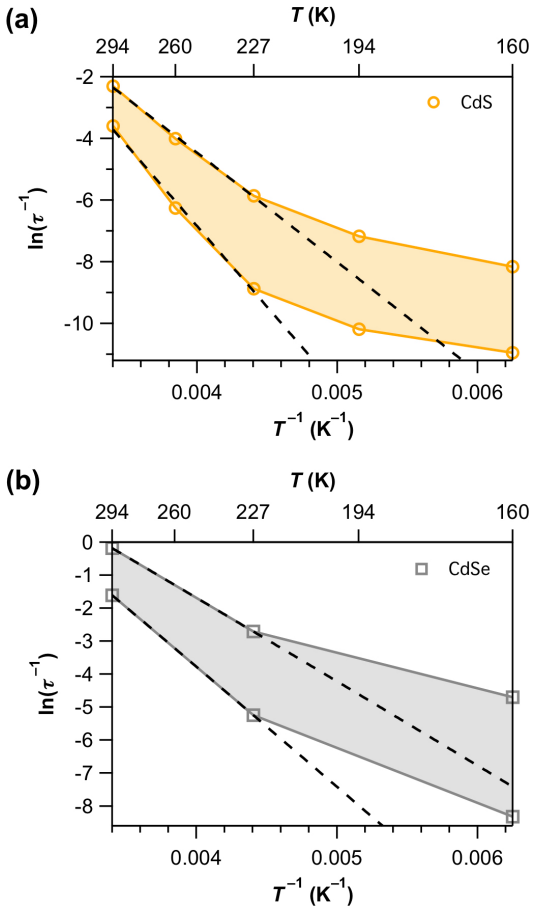

Figure 4. Arrhenius plot of hole-hopping rate in (a) CdS and (b) CdSe NRs. Data is plotted as the natural log of τ^{-1} against T^{-1}, where τ is in units of nanoseconds. Data in the range 227–294 K is fitted with the expression for classical Marcus theory (black dashed line).

At higher temperatures (227–294 K), the hole-hopping rate exhibits Arrhenius behavior (Figure 4). This result is consistent with previous theoretical calculations, which suggested that the trapped hole undergoes a series of incoherent, thermally-activated hops between trap sites on the nanocrystal surface.[13] In this mechanism, the rate of hole transfer between degenerate trap states at high temperatures is given by classical Marcus theory, $\kappa = \frac{2\pi}{\hbar}|J|^2 \frac{1}{\sqrt{4\pi\lambda k_B T}} \exp(-\lambda/4k_B T)$, where λ is the reorganization energy and $|J|^2$ is the electronic coupling between the initial and final states.[40] In this experiment we are only sensitive to trapped-hole motion along the length of the nanorod,[10] so λ and $|J|^2$ here are specifically associated with chalcogenide-to-chalcogenide hole hopping steps with a component along the wurtzite *c*-axis.[13] The data for the upper and lower bounds of $\tau^{-1}(T)$ in Figure 4 were fit to the expression for classical Marcus theory over the range of 227 to 294 K to find the upper and lower bounds of λ and $|J|^2$. The values of λ come directly from the slope of the Arrhenius plot, giving 1.2–1.9 eV and 1.0–1.4 eV for CdS and CdSe NRs, respectively. We obtain estimates for $|J|^2$ from the intercept of Figure 4 using the wurtzite *c*-axis lattice constants of CdS and CdSe[39] for a and the previous estimates for z_0, which are on the order of 1 nm for both CdS and CdSe NRs.[10,12] This gives estimates for $\sqrt{|J|^2}$ of 20–300 meV and 20–100 meV for CdS and CdSe NRs, respectively. These values for $|J|^2$ and λ in turn give estimates for D at room temperature of 10^{-9}–10^{-7} cm^2 s^{-1} and 10^{-8}–10^{-7} cm^2 s^{-1} for CdS and CdSe NRs,

respectively, and estimates for κ at room temperature of 10^6–10^7 s^{-1} and 10^7–10^8 s^{-1} for CdS and CdSe NRs, respectively. Overall, these results are consistent with theoretical predictions for weak electronic coupling between hole trap sites on nearest and next-nearest neighboring surface sulfur atoms along the length of the CdS NR.[13] The large values of λ found here are similar to calculations for diffusive carrier hopping in some polar semiconductors.[41] The small J/λ ratio indicates that the trapped holes form nonadiabatic small polarons that are highly localized on surface chalcogenide atoms and coupled strongly to phonons,[13,42] which leads to slow diffusion compared to band-edge carrier diffusion for these materials in the bulk.

At low temperatures, a fundamentally different regime of hole hopping emerges. In the range of 160 to 227 K, high-temperature classical Marcus theory breaks down and the hole-hopping rate depends more weakly on temperature (Figure 4). This behavior, together with the large estimated values of λ at higher temperatures, suggests that phonon-assisted tunneling plays an important role in trapped-hole diffusion at low temperature, and that hole hopping would be better described in the semiclassical Marcus-Jortner formulation.[43] These results are consistent with studies of trapping and detrapping in CdS and CdSe nanocrystals by low-temperature photoluminescence spectroscopy, which also suggest strong trapped carrier–phonon coupling.[6] However, quantitative modeling of trapped hole–phonon coupling using the present data is not trivial because the trapped hole may couple to a broad spectrum of bath modes made up of multiple lattice phonons and ligand vibrations.[44] Theoretical calculations are needed to map out the lattice and ligand modes that couple to trapped-hole hopping on the surfaces of CdS and CdSe nanocrystals. Our findings highlight that high-temperature Marcus theory limit may not be sufficient to understand low-temperature excited-state processes in nanocrystals.

In conclusion, this work addressed the fundamental understanding of excited-state dynamics of trapped photoexcited holes in CdS and CdSe nanocrystals. The data strongly support a model of trapped-hole diffusion, while several alternative mechanisms for power-law recombination dynamics that rely on thermally-activated decay pathways are ruled out. The temperature-dependent TA data provide quantitative insights about trapped-hole diffusion, showing that electronic coupling between neighboring trap states is weak while trapped holes couple strongly to phonons, making diffusion a slow process. Moreover, the data indicate that trap-to-trap hole hopping behaves classically at room temperature but point to a semiclassical description at low temperatures. The notion that surface-trapped holes are mobile in these nanocrystals and are governed by a semiclassical picture may provide a novel framework for the design of systems that seek to utilize trapped charge carriers for optoelectronic applications.

METHODS

Complete synthetic and experimental details appear in the Supporting Information. From measurements of the TEM images (Figure S1), we estimate that the CdS NRs studied have average rod diameters of 4.8 ± 0.4 nm, bulb diameters of 5.8 ± 0.8 nm, and lengths of 32 ± 3 nm, while for the CdSe NRs the average rod diameters are 8.1 ± 0.8 nm, the bulbs are 9.6 ± 1.2 nm, and the lengths are 39 ± 4 nm. All TA experiments were performed on nanocrystals that were functionalized with 3-mercaptopropanoic acid (3-MPA) and suspended in a glass-forming solvent mixture of 4:1 ethanol:methanol (v/v) at an optical density of ~1 at the lowest-energy absorption peak (Figure S6). The concentration of CdS and CdSe NRs used for TA experiments was about 100 nM. The sample was held in a 1 cm cryogenic cuvette equipped with a screw cap. Samples were prepared under Ar in a glovebox then immediately moved to the cryostat, which was promptly purged with nitrogen. The pump beam was passed through a depolarizer and the power

was controlled with neutral density filters. The pump beam had a beam waist of ~240 μm, pulse duration of ~150 fs, and pulse energy of 20 nJ/pulse for 400 nm excitation of the CdS NRs and 6 nJ/pulse for 600 nm excitation of the CdSe NRs. The pump powers in all cases were chosen such that the TA decay trace shapes were independent of pump power at both 294 K and 160 K so that the signal originated primarily from nanocrystals excited by a single photon.[45]

The rod and bulb decay traces were obtained by spectral averaging over the appropriate regions that isolate their signals,[10,12] accounting for the spectral shift with changing temperature. For CdS nanorods, time traces of the rod signal at 294, 260, 227, 194 and 160 K were obtained by averaging signal over the spectral windows 435–437, 434–436, 434–436, 434–436 and 433–435 nm, respectively, and the time traces of the bulb signal were obtained by averaging over 464–484, 467–476, 470–490, 478–488 and 480–490 nm, respectively. For CdSe nanorods, time traces of the rod signal at 294, 227 and 160 K were obtained by averaging signal over the spectral windows 628–629, 622–624 and 620–621 nm, respectively, and the time traces of the bulb signal were obtained by averaging signal over 665–675, 675–690 and 690–700 nm, respectively. To obtain the power-law exponents given in Figure 3, the power-law tails of the decay traces in Figure 2c,d were fit between the onset of the power law and the end of the experimental time window (400 μs). The onset of the power-law tails were determined by iteratively fitting the end of the decay to a power-law function and checking the reduced chi-squared values, progressively moving the onset to earlier times in each iteration until the reduced chi-squared values increased by 5% above the minimum value found. TA traces were smoothed using a Savitzky-Golay filter because this method preserves higher order moments of the signal.[46] Fitting was performed on raw data and the data was smoothed for presentation only.

ACKNOWLEDGMENTS

CdS nanorod synthesis was supported by the U.S. Department of Energy, Office of Science, Office of Basic Energy Sciences, Division of Chemical Sciences, Geosciences and Biosciences, through the National Renewable Energy Laboratory under Contract No. DE-AC36-08GO28308. CdSe nanorod synthesis was supported by the U.S. Department of Energy, Office of Basic Energy Sciences, Division of Materials Sciences and Engineering under Award No. DE-SC0010334. TA spectroscopy, data analysis, and modeling were supported by the Air Force Office of Scientific Research under AFOSR Award No. FA9550-15-1-0253 and the National Science Foundation Graduate Research Fellowship under Grant No. DGE 1144083 (J. K. U.). J. D. E. acknowledges support from the National Science Foundation under grant No. CHE-1455365. We thank Niels Damrauer for loan of the cryostat and Ryan Dill for assistance in its use.

REFERENCES

1. Ekimov, A. I.; Onushchenko, A. A., Quantum size effect in three-dimensional microscopic semiconductor crystals. *J. Exp. Theor. Phys. Lett.,* **1981,** *34*, 345-349.
2. Choi, C. L.; Alivisatos, A. P., From artificial atoms to nanocrystal molecules: Preparation and properties of more complex nanostructures. *Annu. Rev. Phys. Chem.,* **2010,** *61*, 369-389.
3. Klimov, V. I.; Schwarz, C. J.; McBranch, D. W.; Leatherdale, C. A.; Bawendi, M. G., Ultrafast dynamics of inter- and intraband transitions in semiconductor nanocrystals: Implications for quantum-dot lasers. *Phys. Rev. B,* **1999,** *60*, R2177-R2180.
4. Jones, M.; Scholes, G. D., On the use of time-resolved photoluminescence as a probe of nanocrystal photoexcitation dynamics. *J. Mater. Chem.,* **2010,** *20*, 3533-3538.

5. Knowles, K. E.; McArthur, E. A.; Weiss, E. A., A multi-timescale map of radiative and nonradiative decay pathways for excitons in CdSe quantum dots. *ACS Nano,* **2011,** *5*, 2026-2035.
6. Mooney, J.; Krause, M. M.; Saari, J. I.; Kambhampati, P., A microscopic picture of surface charge trapping in semiconductor nanocrystals. *J. Chem. Phys.,* **2013,** *138*, 204705.
7. McBride, J. R.; Pennycook, T. J.; Pennycook, S. J.; Rosenthal, S. J., The possibility and implications of dynamic nanoparticle surfaces. *ACS Nano,* **2013,** *7*, 8358-8365.
8. Peterson, M. D.; Cass, L. C.; Harris, R. D.; Edme, K.; Sung, K.; Weiss, E. A., The role of ligands in determining the exciton relaxation dynamics in semiconductor quantum dots. *Annu. Rev. Phys. Chem.,* **2014,** *65*, 317-339.
9. Krause, M. M.; Kambhampati, P., Linking surface chemistry to optical properties of semiconductor nanocrystalsl. *Phys. Chem. Chem. Phys.,* **2015,** *17*, 18882-18894.
10. Utterback, J. K.; Grennell, A. N.; Wilker, M. B.; Pearce, O.; Eaves, J. D.; Dukovic, G., Observation of trapped-hole diffusion on the surfaces of CdS nanorods. *Nat. Chem.,* **2016,** *8*, 1061-1066.
11. Grennell, A. N.; Utterback, J. K.; Pearce, O. M.; Wilker, M. B.; Dukovic, G., Relationships between exciton dissociation and slow recombination within ZnSe/CdS and CdSe/CdS dot-in-rod heterostructures. *Nano Lett.,* **2017,** *17*, 3764-3774.
12. Utterback, J. K.; Hamby, H.; Pearce, O.; Eaves, J. D.; Dukovic, G., Trapped-hole diffusion in photoexcited CdSe nanorods. *J. Phys. Chem. C,* **2018,** *122*, 16974-16982.
13. Cline, R. P.; Utterback, J. K.; Strong, S. E.; Dukovic, G.; Eaves, J. D., On the nature of trapped-hole states in CdS nanocrystals and the mechanism of their diffusion. *J. Phys. Chem. Lett.,* **2018,** *9*, 3532-3537.
14. Wu, K.; Du, Y.; Tang, H.; Chen, Z.; Lian, T., Efficient extraction of trapped holes from colloidal CdS nanorods. *J. Am. Chem. Soc.,* **2015,** *137*, 10224-10230.
15. Olshansky, J. H.; Balan, A. D.; Ding, T. X.; Fu, X.; Lee, Y. V.; Alivisatos, A. P., Temperature-dependent hole transfer from photoexcited quantum dots to molecular species: Evidence for trap-mediated transfer. *ACS Nano,* **2017,** *11*, 8346-8355.
16. Li, Q. Y.; Zhao, F. J.; Qu, C.; Shang, Q. Y.; Xu, Z. H.; Yu, L.; McBride, J. R.; Lian, T. Q., Two-dimensional morphology enhances light-driven H_2 generation efficiency in CdS nanoplatelet-Pt heterostructures. *J. Am. Chem. Soc.,* **2018,** *140*, 11726-11734.
17. Wei, H. H. Y.; Evans, C. M.; Swartz, B. D.; Neukirch, A. J.; Young, J.; Prezhdo, O. V.; Krauss, T. D., Colloidal semiconductor quantum dots with tunable surface composition. *Nano Lett.,* **2012,** *12*, 4465-4471.
18. Wu, K.; Zhu, H.; Liu, Z.; Rodriguez-Cordoba, W.; Lian, T., Ultrafast charge separation and long-lived charge separated state in photocatalytic CdS-Pt nanorod heterostructures. *J. Am. Chem. Soc.,* **2012,** *134*, 10337-10340.
19. Jasieniak, J.; Mulvaney, P., From Cd-rich to Se-rich–the manipulation of CdSe nanocrystal surface stoichiometry. *J. Am. Chem. Soc.,* **2007,** *129*, 2841-2848.
20. Keene, J. D.; McBride, J. R.; Orfield, N. J.; Rosenthal, S. J., Elimination of hole-surface overlap in graded CdS_xSe_{1-x} nanocrystals revealed by ultrafast fluorescence upconversion spectroscopy. *ACS Nano,* **2014,** *8*, 10665-10673.
21. Houtepen, A. J.; Hens, Z.; Owen, J. S.; Infante, I., On the origin of surface traps in colloidal II-VI semiconductor nanocrystals. *Chem. Mater.,* **2017,** *29*, 752-761.
22. Kern, S. J.; Sahu, K.; Berg, M. A., Heterogeneity of the electron-trapping kinetics in CdSe nanoparticles. *Nano Lett.,* **2011,** *11*, 3493-3498.

23. Rabouw, F. T.; Kamp, M.; van Dijk-Moes, R. J. A.; Gamelin, D. R.; Koenderink, A. F.; Meijerink, A.; Vanmaekelbergh, D., Delayed exciton emission and its relation to blinking in CdSe quantum dots. *Nano Lett.,* **2015,** *15*, 7718-7725.
24. Rabouw, F. T.; van der Bok, J. C.; Spinicelli, P.; Mahler, B.; Nasilowski, M.; Pedetti, S.; Dubertret, B.; Vanmaekelbergh, D., Temporary charge carrier separation dominates the photoluminescence decay dynamics of colloidal CdSe nanoplatelets. *Nano Lett.,* **2016,** *16*, 2047-2053.
25. Kuno, M.; Fromm, D. P.; Hamann, H. F.; Gallagher, A.; Nesbitt, D. J., "On"/"off" fluorescence intermittency of single semiconductor quantum dots. *J. Chem. Phys.,* **2001,** *115*, 1028-1040.
26. Redner, S., *A guide to first-passage processes*. Cambridge University Press: Cambridge, **2001**.
27. Wu, K. F.; Rodriguez-Cordoba, W. E.; Liu, Z.; Zhu, H. M.; Lian, T. Q., Beyond band alignment: Hole localization driven formation of three spatially separated long-lived exciton states in CdSe/CdS nanorods. *ACS Nano,* **2013,** *7*, 7173-7185.
28. Wu, K.; Rodriguez-Cordoba, W.; Lian, T., Exciton localization and dissociation dynamics in CdS and CdS-Pt quantum confined nanorods: Effect of nonuniform rod diameters. *J. Phys. Chem. B,* **2014,** *118*, 14062-14069.
29. Rudin, S.; Reinecke, T. L.; Segall, B., Temperature-dependent exciton linewidths in semiconductors. *Phys. Rev. B,* **1990,** *42*, 11218-11231.
30. Mack, T. G.; Jethi, L.; Kambhampati, P., Temperature dependence of emission line widths from semiconductor nanocrystals reveals vibronic contributions to line broadening processes. *J. Phys. Chem. C,* **2017,** *121*, 28537-28545.
31. Grimaldi, G.; Geuchies, J. J.; van der Stam, W.; du Fossé, I.; Brynjarsson, B.; Kirkwood, N.; Kinge, S.; Siebbeles, L. D. A.; Houtepen, A. J., Spectroscopic evidence for the contribution of holes to the bleach of Cd-chalcogenide quantum dots. *Nano Lett.,* **2019**, DOI: 10.1021/acs.nanolett.9b00164.
32. Reid, K. R.; McBride, J. R.; La Croix, A. D.; Freymeyer, N. J.; Click, S. M.; Macdonald, J. E.; Rosenthal, S. J., Role of surface morphology on exciton recombination in single quantum dot-in-rods revealed by optical and atomic structure correlation. *ACS Nano,* **2018,** *12*, 11434-11445.
33. Utterback, J. K.; Wilker, M. B.; Mulder, D. W.; King, P. W.; Eaves, J. D.; Dukovic, G., Quantum efficiency of charge transfer competing against nonexponential processes: The case of electron transfer from CdS nanorods to hydrogenase. *J. Phys. Chem. C,* **2019,** *123*, 886-896.
34. Marchioro, A.; Whitham, P. J.; Knowles, K. E.; Kilburn, T. B.; Reid, P. J.; Gamelin, D. R., Tunneling in the delayed luminescence of colloidal CdSe, Cu^{+}-doped CdSe, and $CuInS_2$ semiconductor nanocrystals and relationship to blinking. *J. Phys. Chem. C,* **2016,** *120*, 27040-27049.
35. Whitham, P. J.; Knowles, K. E.; Reid, P. J.; Gamelin, D. R., Photoluminescence blinking and reversible electron trapping in copper-doped CdSe nanocrystals. *Nano Lett.,* **2015,** *15*, 4045-4051.
36. Tsui, E. Y.; Carroll, G. M.; Miller, B.; Marchioro, A.; Gamelin, D. R., Extremely slow spontaneous electron trapping in photodoped n-type CdSe nanocrystals. *Chem. Mater.,* **2017,** *29*, 3754-3762.

37. Chestnoy, N.; Harris, T. D.; Hull, R.; Brus, L. E., Luminescence and photophysics of CdS semiconductor clusters - the nature of the emitting electronic state. *J. Phys. Chem.,* **1986,** *90*, 3393-3399.
38. Baker, D. R.; Kamat, P. V., Tuning the emission of CdSe quantum dots by controlled trap enhancement. *Langmuir,* **2010,** *26*, 11272-11276.
39. Madelung, O., *Semiconductors—Basic Data*. 2nd ed.; Springer: Berlin, **1996**.
40. Marcus, R. A.; Sutin, N., Electron transfers in chemistry and biology. *Biochim. Biophys. Acta,* **1985,** *811*, 265-322.
41. Deskins, N. A.; Dupuis, M., Electron transport via polaron hopping in bulk TiO_2: A density functional theory characterization. *Phys. Rev. B,* **2007,** *75*, 195212.
42. Alexandrov, A. S.; Mott, S. N., *Polarons & Bipolarons*. World Scientific: Singapore, **1995**.
43. Jortner, J., Temperature-dependent activation-energy for electron-transfer between biological molecules. *J. Chem. Phys.,* **1976,** *64*, 4860-4867.
44. Beecher, A. N.; Dziatko, R. A.; Steigerwald, M. L.; Owen, J. S.; Crowther, A. C., Transition from molecular vibrations to phonons in atomically precise cadmium selenide quantum dots. *J. Am. Chem. Soc.,* **2016,** *138*, 16754-16763.
45. Klimov, V. I., Spectral and dynamical properties of multilexcitons in semiconductor nanocrystals. *Annu. Rev. Phys. Chem.,* **2007,** *58*, 635-673.
46. Press, W. H.; Teukolsky, S. A.; Vetterling, W. T.; Flannery, B. P., *Numerical Recipes: The Art of Scientific Computing*. 3rd ed.; Cambridge University Press: Cambridge, **2007**.